University of Sistan and Baluchestan

Challenges in Nano and Micro Scale Science and Technology

Online ISSN: 2821 - 000X

Electrochemical Approach for The In-Situ Synthesis of a Poly(Sulfosalicylic Acid)/Nickel Oxide Nanoparticles/MCM-41 Nanocomposite for Guanine Detection

Shiva Alipour[1] | Majid Arvand[2]✉ | Akram Pourhabib[3]

1. Department of Chemistry, Pardis Campus, University of Guilan, Park-e-Shahr, P.O. Box 4199613776, Rasht, Iran
2. Corresponding Author, Electroanalytical Chemistry Laboratory, Faculty of Chemistry, University of Guilan, Namjoo Street, P.O. Box: 1914–41335, Rasht, Iran. Email: arvand@guilan.ac.ir
3. Education Organization of Guilan Province, Farhang Square, P.O. Box: 41849-83111, Rasht

Article Info

Article type:
Research Article

Keywords:
DNA sample,
Electropolymerization,
Guanine,
NiO-MCM-41 nanocomposite,
Poly(5-sulfosalicylic acid).

ABSTRACT

Guanine, a purine base in deoxyribonucleic acid (DNA), has a low redox potential, making it susceptible to oxidation and contributing to DNA damage and mutations. In the current study, a new polymer nanocomposite consisting of nickel oxide-Mobile crystalline material-41 (NiO-MCM-41) nanocomposites and poly(5-sulfosalicylic acid) (PSSA) was prepared by electropolymerization for modification of the graphite/glassy carbon electrode (Gr/GCE) surface and sensitive measurement of the guanine. The synthesized nanocomposite was identified and confirmed by FE-SEM, EDX and FT-IR techniques. The electrochemical behavior of guanine on the surface of the PSSA/NiO-MCM-41/Gr/GCE was analyzed in optimal conditions using cyclic voltammetry (CV) and differential pulse voltammetry (DPV) methods. The proposed modified electrode achieved a satisfactory dynamic range between the anodic peak current and the concentration of guanine, with a linear range of 0.001–36 µM, a sensitivity of 0.977 µA/µM, and the detection limit (LOD) was determined to be 0.5 nM (signal/noise = 3). This sensor was successfully used in the determination of guanine in the real sample of fish sperm's DNA.

INTRODUCTION

DNA, a double-helix biomacromolecule, stores hereditary genetic information and facilitates protein synthesis [1,2]. Its structure comprises nitrogenous bases (adenine, guanine [purines], cytosine, thymine [pyrimidines]), deoxyribose sugar, and phosphate groups. These bases serve as fundamental building blocks [3,4]. Abnormal concentrations disrupt enzymatic catabolic/anabolic pathways and metabolic interconversions, leading to diseases like cancer, HIV, and epilepsy through mutated purine-pyrimidine metabolism [5–9]. Therefore, the evaluation of concentration levels of purine bases is considered to be a significant parameter in physiology and clinical pathology [10]. In this regard, increasing consideration of researchers is given to the progress of a straightforward, rapid, sensitive and precise analytical procedure for the detection and designation of these bases in DNA, particularly from the view of superior understanding of the mechanism of replication and destruction processes in the DNA skeleton [11]. Up to now, various analytical methodologies such as mass spectrometry [12], high performance liquid chromatography (HPLC) [13], capillary electrophoresis (CE) [14] and gas chromatography [15] have been developed for the analysis of purine bases in nucleic acids. However, these mentioned methods can be employed for sensitive designation of guanine, but they have some disadvantages such as time-consuming, approximately expensive, light sensitivity, and complicated pre-treatment [12,16,17]. Therefore, they are not appropriate for real-time determination series [18]. To prevail over these restriction, electrochemical techniques seem to be a suitable successor owing to their supremacies such as swift response, inherent simplicity, cost-effective assay, miniaturization and facile compatibility for in-situ analysis [19,20]. However, the use of electrochemical sensors to detect guanine immediately in the real samples mostly confronts some

How to Cite this paper: Alipour Sh, Arvand M, Pourhabib A. Electrochemical Approach for The In-Situ Synthesis of a Poly(Sulfosalicylic Acid)/Nickel Oxide Nanoparticles/MCM-41 Nanocomposite for Guanine Detection. *Challenges in Nano and Micro Scale Science and Technology*. 2023; 11(2): 40-51. DOI: 10.22111/cnmst.2025.51292.1258

© Alipour Sh, Arvand M, Pourhabib A.
Publisher: University of Sistan and Baluchestan.
DOI: 10.22111/cnmst.2025.51292.1258

problems. Owing to low electron transfer capacity and limited active surface areas, the response for the direct oxidation of guanine was insignificant on the conventional unmodified electrode surfaces [21], which leads to low sensitivity and poor reproducibility. In order to dissolve the mentioned problems, the modified electrodes are predominantly used as alternative procedure [22]. Modification of the sensing layer composition for distinctive interactions with analytes is an essential step in design of the practical voltammetric sensor. For example, Jeevagan et al. fabricated a self-assembled monolayer of 1,8,15,22-tetraaminophthalocyanatonickel(II) modified GCE for the detection of guanine [23]. Geng et al. developed a biosensor for the simultaneous determination of guanine and adenine based on overoxidized polypyrrole/multiwalled carbon nanotube and molybdenum disulfide modified GCE [24]. Ferancová et al. constructed pearl-like CdS microspheres modified GCE and combined with the advantages of good biocompatibility of chitosan to detect guanine and adenine [25]. Kodakat et al. fabricated a molecularly imprinted polymer based voltammetric sensor for guanine by electropolymerization of the functional monomer phenol in presence of guanine onto the surface of a *poly*(L- glutamic acid) modified GCE [26]. Huang et al. fabricated an electrochemical sensor on the basis of the carboxylic acid functionalized graphene for the simultaneous detection of guanine and adenine [27]. Liu et al. prepared a PbO_2-carbon nanotubes-room temperature ionic liquid composite film modified GCE to investigate the electrochemical oxidation behavior of guanine and adenine [28]. Tang et al. synthesized a novel composite film which contained multi-walled carbon nanotubes incorporated poly new fuchsin for the simultaneous detection of guanine, adenine and thymine [29].

Nanotechnology has become a leading field in analytical chemistry, with nanoparticles playing a crucial role [30]. Metal nanoparticles, in particular, are valued for their electronic, optical, and catalytic properties, making them ideal for electrochemical sensors and biosensors. They enhance electron transfer and catalyze reactions due to their superior conductivity [31–33]. Metal oxides, such as nickel oxide, offer semiconductor properties and are noted for their stability and electrocatalytic capabilities [34]. Additionally, silica-based mesoporous materials are gaining attention due to their uniform channels, large surface area, and potential to enhance electron transfer reactions, thereby improving electrochemical sensitivity [35,36]. Pure MCM-41, characterized by a hexagonal array of unidirectional pore structures, is neutral in charge and exhibits only weak hydrogen-bonding sites, which limits its application in sensing. However, the integration of MCM-41 with NiO nanoparticles to form a porous magnetic nanocomposite presents significant opportunities for practical applications [37,38]. Additionally, polymer/nanomaterial composites have been extensively studied due to their potential to create new materials that combine the properties of each component synergistically. Incorporating nanocomposites into polymer films can lead to enhanced performance in specific applications [39].

Relying on all these distinguished reasons, our study endeavors to introduce an electrochemical sensor tailored for the precise quantification of detection of guanine molecules, particularly in DNA samples. This sensor is meticulously crafted through the process of electropolymerization, whereby the PSSA/NiO/MCM-41 nanocomposite is strategically deposited onto the surface of a Gr/GCE substrate. The resultant PSSA/NiO/MCM-41/Gr/GCE electrochemical sensor manifests an outstanding performance in detecting guanine, characterized by heightened sensitivity and selectivity, rapid response kinetics, and commendable levels of reproducibility and repeatability. The synergistic amalgamation of PSSA/NiO/MCM-41 nanocomposite with the Gr/GCE platform not only enhances the sensing capabilities but also facilitates efficient electrochemical processes. This is attributed to the optimized interaction between the composite material and the electrode surface, which promotes enhanced loading of electrochemical species and facilitates expedited electron transfer kinetics. Additionally, until the time of this study, no research has reported the detection of guanine using the PSSA/NiO/MCM-41/Gr/GCE structure, thus making this study a novel research basis in this field.

EXPERIMENTAL

Regents and Materials

All reagents and solvents were of the highest purity from Merck (Darmstadt, Germany) and were used without further purification. Nickel(II) chloride ($NiCl_2$), sulfosalicylic acid (SSA), graphite powder (Gr), hydrochloric acid (HCl), ethanol (C_2H_5OH) and isopropanol (C_3H_8O) were obtained from Merck Company (Darmstadt, Germany). Guanine was acquired from Sigma-Aldrich (Saint Louis, USA). The MCM-41material, with a pore diameter of 36.61 Å, a pore volume of 1.14 cm^3/g, and a surface area of 1022 m^2/g, was obtained from Plasma Chem. GmbH (Berlin, Germany). Phosphate buffer solution (0.1 M) was prepared by mixing solutions of 0.1 M phosphoric acid (H_3PO_4) and 0.1 M sodium hydroxide (NaOH) over the pH range of 3–9. Fish sperm was achieved from Agricultural Biotechnology Research Institute of Iran-North Branch (ABRII). In this study, all solutions were catered with deionized (DI) water.

Apparatus

All the electrochemical determinations were done by the PalmSens electrochemical analyzer (Houten, Netherlands) and controlled by PS-Trace 4.5 software. A conventional three-electrode system, including a modified electrode as working electrode, an Ag/AgCl saturated in potassium chloride as reference electrode and platinum role as counter electrode were utilized to receive the electrochemical data. All electrochemical investigations were carried out at ambient temperature. All the solutions' pH values were evaluated by a

Metrohm pH meter (model 827, Herisau, Switzerland). The field emission scanning electron microscopy (FE-SEM; Sigma, Carl Zeiss, Germany) measurements was employed to recorded morphological images of modified electrode. The chemical composition was obtained using energy dispersive X-ray spectroscopy (EDX; Sigma, Carl Zeiss, Germany). The structure of polymer was investigated by a Fourier transform infrared spectrometer (FT–IR; Shimadzu 8900, Kyoto, Japan) at a standard resolution of 8 cm^{-1} within the 4000–400 cm^{-1} range.

PSSA/NiO/MCM-41 Polymer Nanocomposite Synthesis

To synthesize this nanocomposite, first, 0.1 g of nickel chloride green salt ($NiCl_2$) was dissolved in 25 mL DI water. For having a uniform solution, the prepared solution was magnetically stirred. Then, 0.5 g of the mesoporous compound MCM-41 was poured into the solution containing nickel chloride and put the obtained solution in the ultrasonic bath for 15 minutes to allow the zeolite compound is fully dispersed in the solution. After that, the solution was put on the magnetic stirrer for 6 hours at the ambient temperature to be stirred properly. For preparation of sample solutions, 0.1 M NaOH was used to obtain pH=8. In this phase, the solution turned into a greenish gel. The obtained gel was again put on the magnetic stirrer for another 6 hours at the laboratory temperature, and then, the obtained mixture was withdrawn and put in the laboratory environment for 10 hours. It is the so-called 'aging' of the gel. After 10 hours, the sediments were separated by centrifuging at 12,000 rpm for 10 minutes, and rinsed by DI water several times. Then, the obtained sediments were dried at a temperature of 80 °C in the oven available in the laboratory, for 24 hours. Finally, the obtained powder was put in stove with a temperature of 550 °C and a heating rate of 2 °C/min for 2 hours. In this phase, sand-like blackish powder was synthesized which is a composite of nickel-coated nanoparticles in a bed of MCM-41 zeolite.

In the next step, 0.0642 g of SSA monomer was mixed with phosphate buffer solution with pH=5.5 in a volumetric flask with 25 mL volume, then a transparent and uniform solution was obtained. Then, 0.002 g of the synthesized black powder which was obtained from the previous phase was taken and mixed with 20 mL of 5-sulfosalicylic acid. To preparation the uniform solution, this compound was put in the ultrasonic bath for 15 to 20 minutes. This darkish solution was used as the polymerization solution in all phases of the experiment.

Preparation of the Modified Electrodes

The glassy carbon electrode was polished with alumina powder to obtain a mirror-like surface. Then, the electrode was put inside a DI water/ethanol (1:1) solution and this solution was put in the ultrasonic bath for 3 minutes and allowed to dry at room temperature. The working electrode used was prepared by the drop method. Firstly, 0.01 g of graphite powder was mixed with 10 mL of dimethylformamide (DMF) and Nafion and put in the ultrasonic bath to obtain a homogenous solution. Then, 6 µL of this suspension (1 mg/mL) was put on the polished glassy carbon electrode surface and was dried in the ambient temperature. This electrode is recognized as Gr/GCE. The glassy carbon electrode which modified with graphite was sunk in the polymerization solution for electropolymerization process using CV in optimal conditions (potential ranging between -1 to 2 V *vs.* Ag/AgCl at a scan rate of 0.1 V/s for 10 cycles of potential). This electrode is recognized as PSSA/NiO/MCM-41/Gr/GCE (Fig. 1). Prior to each measurement, the obtained modified electrode was cleaned by the use of CV from -1 to 2 V at 0.1 V/s for two scans in the phosphate buffer solution with pH = 7 to remove the monomer and the species that were absorbed physically. All modified glassy carbon electrodes such as Gr/GCE, 5-sulfosalicylic acid/GCE, MCM-41/GCE, and NiO-MCM-41/GCE were evaluated by the above method.

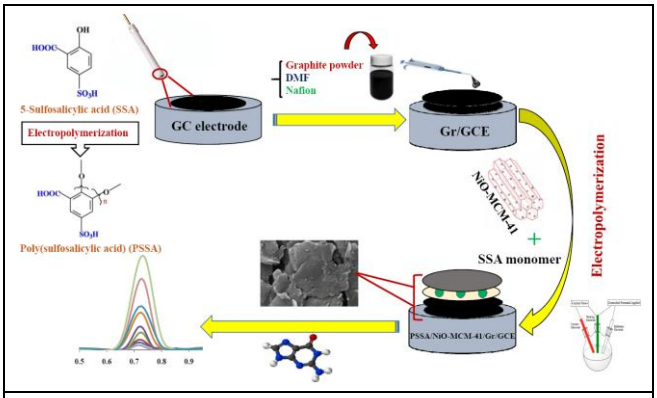


Fig. 1. Schematic representation of in situ electrochemical synthesis of PSSA/NiO-MCM-41/Gr/GCE.

Real Samples Preparation

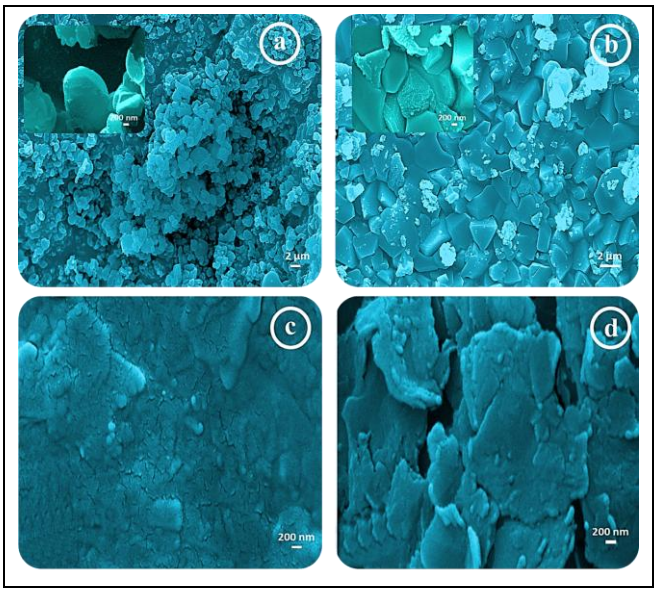
Firstly, a 75% ethanol solution was prepared and put in the refrigerator. Then, 1 mL of the DNG reagent was poured into the test tube and shaken for 20 minutes. 200 µL of fish sperm was obtained and 1 mL of DNG reagent was added to it. Then again, it was shaken for 20 min to obtain completely homogeneous (biphasic) solution. In the following, the accumulated solid materials were removed in case of existence. Afterward, 100 µL of isopropanol was added to the solution containing the fish sperm and it was shaken and the obtained complex was put into the freezer for 20 min. After removal of the solution from the freezer, the separation was done by a centrifuge at 12,000 rpm for 15 minutes. The solution on the top of the sediments was extracted and 2 mL of cold 75% ethanol was added to the sediments, and it was put inside the centrifuge for another 5 minutes. After the separation of the solution available on the top of the sediments, it was discharged and the obtained sediments were put in an oven with a temperature of 65 °C for 5 minutes to be completely dried. By the above phases, the DNA of the fish sperm was extracted. The obtained DNA was dissolved in 100 µL of deionized water and shaken intensely by hand and was again put inside the oven for 5 minutes. To destroy the DNA and measure the guanine in its structure, the following steps must be done: An amount of 1 mL of 1 M HCl was added to the extracted

DNA and it was put inside the hot water bath for 60 minutes. After 60 minutes, the solution was quickly transferred to the cold water bath to be kept there for 10 minutes. In order to neutralize the solution, 1 mL of 1 M NaOH was used. Then, by phosphate buffer solution (pH=5), the obtained complex increased to 10 mL volume.

RESULTS AND DISCUSSION

Characterization

The surface morphology of the modified electrodes was analyzed by FE-SEM due to the physical morphology affected on the response of an electrochemical sensor. Fig. 2(a) demonstrates the image of MCM-41 before modification with NiO nanoparticles. The synthesized MCM-41 has a porous surface which leads to develop on electrode surface area. In addition, magnified MCM-41 surface showed that the size of the pores is in micro-scale. Fig. 2(b) shows the modified MCM-41 by NiO nanoparticles. The NiO nanoparticles are well placed on the inner surface of the MCM-41 pores. As is seen in the NiO/MCM-41 background image, the NiO crystals are grown and created a very rough, rugged, and porous surface in the MCM-41 pores, which lead to a significant increase the surface area. Fig. 2(c) displays the image of the modified electrode with the PSSA polymer and Fig. 2(d) shows the modified electrode by PSSA/NiO/MCM-41/Gr polymer nanocomposite. As is seen in the two images, both modified electrodes have a layered surface, but the Fig. 2(d) which is the FE-SEM image of the modified electrode with PSSA/NiO/MCM-41/Gr nanocomposite has higher surface area and porosity than the modified electrode with PSSA. It indicates that the nanocomposite accelerate the electron transfer process between solution and the electrode during the electrochemical reactions. In order to further confirm the formation of NiO-MCM-41, EDX technique was carried out along with FE-SEM. Fig. 2(e) illustrates the net MCM-41 and Fig. 2(f) shows the modified MCM-41 with NiO nanoparticles. Based on Fig. 2(f), it is cleared that the NiO nanoparticles have grown at MCM-41 pores.



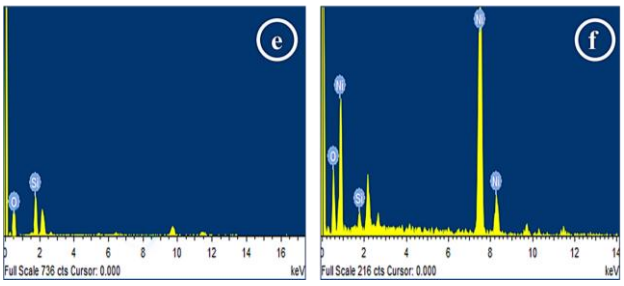


Fig. 2. The FE-SEM image of (a) unmodified MCM-41, (b) MCM-41 modified by NiO nanoparticles, (c) PSSA polymer, (d) polymer modified by NiO/MCM-41 nanocomposite, (**e**) EDX analysis of the net MCM-41, and (f) NiO-MCM-41 nanocomposite.

To prove the formation of the PSSA, the FT-IR technique was used. Fig. 3 shows the FT-IR spectra of SSA monomer (a) and PSSA polymer (b). In Fig. 3(a), the strong absorption peaks around 3405 and 3000 cm^{-1} are for stretching vibrations of O–H functional groups and C–H groups, respectively. Furthermore, in Fig. 3(b), the absorption peaks around 3447, 1383, 1162, 1634, and 1433 cm^{-1} are for the O–H, S=O, and –COO functional groups. This information shows that the PSSA has been created by electropolymerization method using SSA monomer [40].

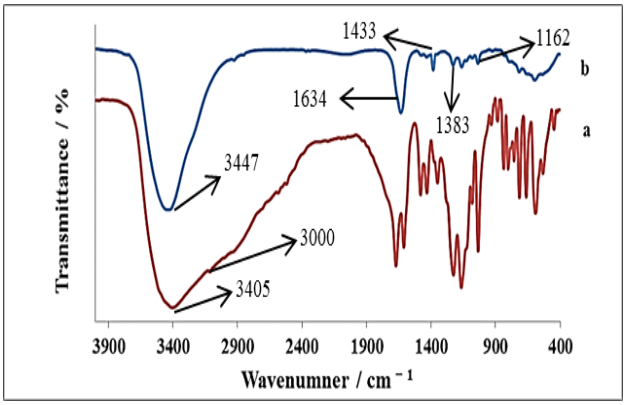


Fig. 3. FT-IR spectra of (a) SSA, and (b) PSSA film

Cyclic voltammetry characterization of modified electrodes

The $K_3[Fe(CN)_6]$ electron transfer reagent with a concentration of 5 mM containing 0.1 M KCl and the CV technique at scan rate of 75 mV/s were used to evaluate the electrochemical behavior of the PSSA/GCE, PSSA/Gr/GCE, and PSSA/NiO/MCM-41/Gr/GCE electrodes. As seen in Fig. 4, all the electrodes have shown a pair of reversible peaks with separation between the cathodic and anodic peak potentials (ΔE_p) which are related to the redox behavior of $K_3[Fe(CN)_6]$. The obtained results from the recorded voltammetry indicate the priority of the modified electrode with the PSSA/NiO/MCM-41 polymer nanocomposite compared to the other electrodes, because this electrode has a higher oxidation current and lower anodic and cathodic peak differences due to presence of PSSA/NiO/MCM-41

polymer nanocomposite, which leads to facilitation of redox process, and improvement of electron transfer rate. The surface area of the different electrodes by CV in 5 mM $K_3[Fe(CN)_6]$ containing 0.1 M KCl was calculated based on the Randles–Sevcik equation for a reversible process [40]:

$$I_{pa}=(2.69 \times 10^5)n^{3/2}D^{1/2}Av^{1/2}C \quad (1)$$

In which I_{pa} is the anodic peak current per A, n is the total number of exchanged electron during the redox process (n=1), D is the diffusion coefficient for $K_3[Fe(CN)_6]$ equal to 7.6×10^{-6} cm^2/s [41], A is the effective area of the electrode surface per cm^2, v is the potential scan rate per V/s, and C is the concentration of $K_3[Fe(CN)_6]$ solution (5×10^{-3} M). By putting the I_{pa} values of each of the electrodes and other values in the equation (1), the PSSA/GCE, PSSA/Gr/GCE, and PSSA/NiO/MCM-41/Gr/GCE electrodes area were calculated as 0.03, 0.116, and 0.158 cm^2, respectively. This increase in the values shows that the presence of PSSA/NiO/MCM-41 polymer nanocomposite leads to an increase in the effective surface area of the electrode (Table S1).

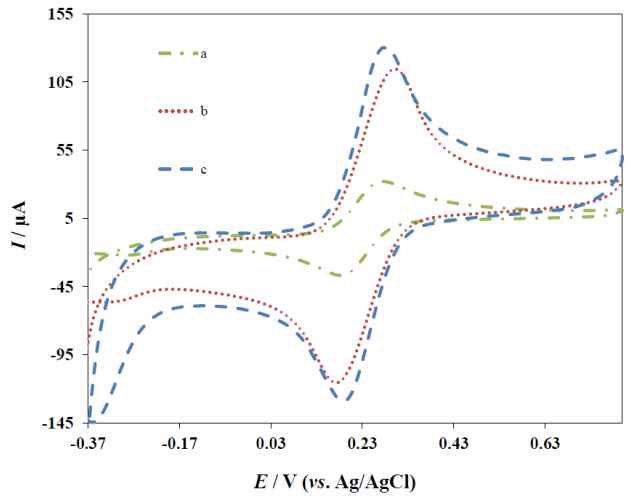


Fig. 4. The cyclic voltammograms obtained from the 0.1 M KCl containing 5 mM $K_3[Fe(CN)_6]$ at the surface of (a) PSSA/GCE, (b) PSSA/Gr/GCE, and (**c**) PSSA/NiO/MCM-41/Gr/GCE with a scan rate of 0.075 V/s.

Electrochemical Behavior of Guanine at the Surface of Different Electrodes

The electrochemical behavior of guanine at various electrode surfaces has been thoroughly investigated using CV, as illustrated in Fig. 5. Cyclic voltammograms were obtained for a 10 µM guanine solution on the surfaces of Gr/GCE, PSSA/GCE, MCM-41/GCE, NiO/MCM-41/GCE, PSSA/Gr/GCE, PSSA/MCM-41/Gr/GCE and PSSA/NiO-MCM-41/Gr/GCE. These experiments aimed to assess the influence of individual components on the electrode response, employing a potential sweep rate of 100 mV/s. The obtained voltammograms revealed that the modified electrode with the PSSA/NiO/MCM-41/Gr polymer nanocomposite did not exhibit any significant electrochemical behavior in the absence of guanine, when tested in a phosphate buffer solution with a pH of 5. However, in the presence of guanine, all the modified electrodes demonstrated an electrochemical response towards the oxidation of the analyte. Upon comparing the electrochemical parameters associated with guanine oxidation on the various modified electrodes, it was observed that the anodic peak current on the electrode modified with the PSSA/NiO/MCM-41/Gr polymer nanocomposite was higher than that of the other electrodes. Specifically, the anodic peak current on the PSSA/NiO/MCM-41/Gr-modified electrode was 1.5 times higher than that of the PSSA/MCM-41/Gr-modified electrode, over 3 times higher than the PSSA/Gr-modified electrode, and almost 1.5 times higher than the PSSA-modified electrode (Table S2). The incorporation of the NiO/MCM-41 nanocomposite into the PSSA/NiO/MCM-41/Gr electrode resulted in an increased surface area, promoting the formation of the polymer and enhancing the number of reactive sites [42]. The synergistic effects arising from the combination of NiO/MCM-41 and PSSA composites facilitated electron transfer, accelerated the kinetic process, and consequently led to heightened sensitivity. Considering the aforementioned findings, the modified electrode featuring the PSSA/NiO/MCM-41/Gr polymer nanocomposite exhibited the most optimal response. Therefore, this electrode was selected for further electrochemical evaluations in subsequent investigations.

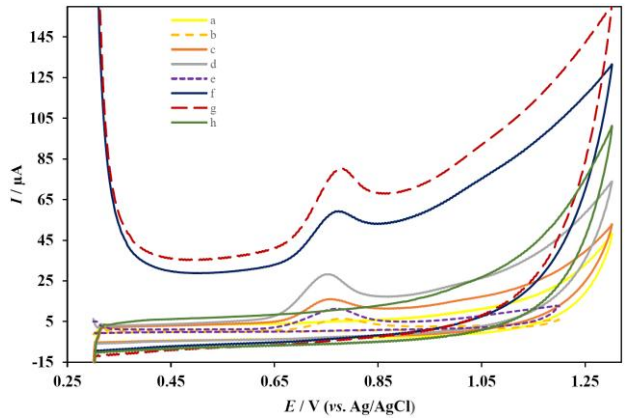


Fig. 5. The cyclic voltammograms of (a) Gr/GCE, (b) PSSA/GCE, (c) MCM-41/GCE, (d) NiO/MCM-41/GCE, (e) PSSA/Gr/GCE, (f) PSSA/MCM-41/Gr/GCE and (g) PSSA/NiO/MCM-41/Gr/GCE in 0.1 M phosphate buffer solution (pH=5.0) containing 10 µM guanine in potential scan rate of 0.1 V/s, and (h) cyclic voltammogram of PSSA/NiO/MCM-41/Gr/GCE in absence of guanine.

Optimization of the Effective Parameters on Guanine Measurement in PSSA/NiO/MCM-41/Gr/GCE Surface

Influence of the number of cycles and scan rates to functional of PSSA for guanine oxidation

To prepare a probe sensitive for the guanine, which includes the polymer film, the iterations and rate of potential scan from the electropolymerization must be optimized because the polymer film thickness directly depends on these two parameters. Therefore, their effects on the proposed electrode were investigated. First, the

iterations of the potential scan in the electropolymerization were changed from 5 to 15, and their current response to 10 µM guanine was investigated. The changes of anodic peak of guanine per changes in iterations of potential scan in Fig. 6(a) show that with the increase in the iterations of potential scan from 5 to 10, the anodic peak current of guanine is initially increased and then decreased. Thus, the optimal iteration for doing the other experiments has been considered as 10. Then, the potential scan rate in the electropolymerization process was changed from 0.03 to 0.07 V/s and the currents responses to 10 µM guanine were investigated. As is seen in the graph in Fig. 6(b), the anodic peak current of guanine is maximized in the potential scan rate of 0.07 V/s. Thus, this value is taken as the optimal value for doing other experiments. Fig. 6 clearly shows the cyclic voltammograms of PSSA formation with optimal values as 10 potential scan iterations and rate of 0.07 V/s in the potential range of -1.0 to 2.0 V on the NiO/MCM-41/Gr surface.

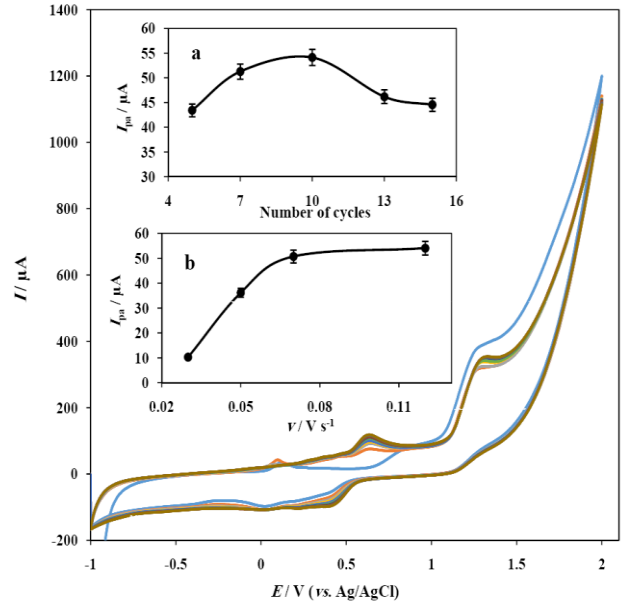


Fig. 6. The cyclic voltammograms of PSSA formation in the presence of 0.1 M phosphate buffer solution (pH=5.0) containing 10 µM of guanine with 10 cycles by scan rate of 0.1 V/s at the surface of PSSA/NiO/MCM-41/Gr/GCE, (a) effect of different numbers of cycles of PSSA formation from 5 to 15 and scan rate of 0.1 V/s, (b) effect of potential scan rate for PSSA formation from 0.03 to 0.12 V/s for 10 cycles.

Influence of buffer type on guanine's electrochemical behavior

The citrate buffer (with pH's 3.5, 4.5, and 6.0), acetate buffer (with pH's 3.5, 4.5, and 6.0), and phosphate buffer (with pH's 3.5, 4.5, and 6.0) with 0.1 M concentration were prepared to select the suitable buffer as the supporting electrolyte for guanine's electrochemical measurement. The CV responses obtained from the modified electrode in each of these solutions with 10 µM concentration of guanine were investigated. In Fig. 7, the cyclic voltammograms recorded in each of the above buffers with pH=4.5 have been provided to compare these three buffers. Based on the obtained results from Table S3, the highest anodic peak current in the guanine oxidation was observed in the phosphate buffer solution. Therefore, the phosphate buffer solution was used as the supporting electrolyte in the future voltammetry measurements.

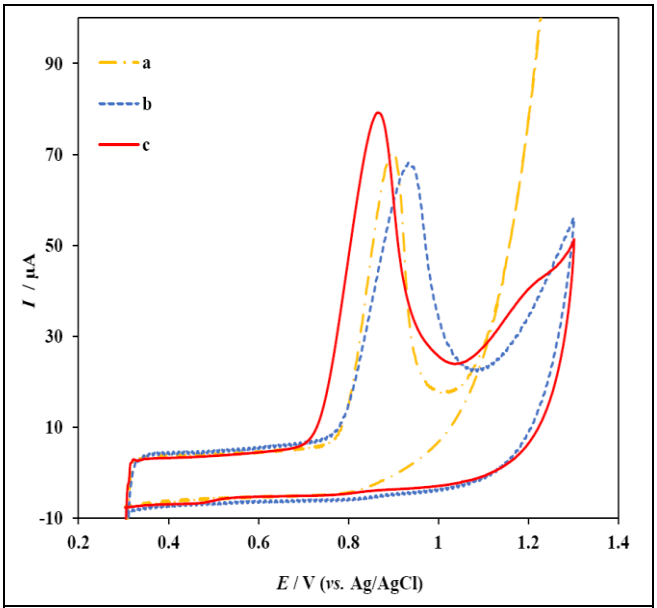


Fig. 7. The cyclic voltammograms of 10 µM guanine oxidation in the buffer solution (a) citrate, (b) acetate, (c) phosphate with pH=4.5 and a scan rate of 0.1 V/s.

Influence of buffer pH

The pH value of supporting electrolyte solution is the effective factor on the peak currents and peak potentials during the guanine oxidation reaction. Since the protons take part in the guanine oxidation process on the modified electrode surface, the oxidation potential depends on the environment's pH. Therefore, to obtain an optimal oxidation current, the optimization of the experiment solution's pH is essential. Phosphate buffer solutions with different pH's were prepared to investigate the effects of pH on the guanine electrochemical response as well as the selection of the optimal pH value. Then, the electrochemical behavior of guanine on the PSSA/NiO/MCM-41/Gr/GCE in the pH range of 3–9 was investigated by the CV technique. The cyclic voltammograms of the guanine oxidation in different pH's have been shown in Fig. S1(a). The results of the anodic peak current *vs.* different pH's and potential changes *vs.* different pH's of guanine are provided in Fig. S1(b) and Fig. S1(c), respectively. Based on Fig. S1(b), it is seen that with the increase in solution's pH, the peak potential moves towards the less positive values, which is indicative of proton's interference in the guanine oxidation reaction. The relationship in peak potential with the pH of the solution at the modified electrode have been shown by the linear regression equation: E_{pa}(V) = -0.0319pH + 0.9809 (R^2=0.9823). The slope of this equation is equal to 0.0319 V, which revealed that the ratio of the number of transferred electrons to the proton number is equal to 2 (half the Nernst equation's slope

value) in the electro-oxidation reaction [43]. Also, Fig. S1(c) shows that the highest anodic peak current is observed in pH=5. Therefore, this pH was selected as the optimal value.

Influence of scanning rate

The effect of scan rate in 0.1 M phosphate buffer solution (pH=5.0) with the presence of 10 µM guanine at the PSSA/NiO/MCM-41/Gr/GCE was verified using CV at various scan rates from 0.01 to 0.18 V/s (Fig. 8). Based on mentioned figure, with the increase in the potential scan rate, the anodic peak current value is increased and the potential peak moves towards the more positive values. Also, as shown in Fig. 8(a), there is a desirable linear relationship between the anodic peak current and the potential scan rate and the corresponding equation can be expressed as $I_{pa}(\mu A) = 354.77v + 5.1507$ (R^2=0.9884), which is a reason behind guanine's reaching to the modified electrode surface in the form of absorption controlled mechanism. Furthermore, as shown well in Fig. 8(b), there is a linear relationship between the logarithmic anodic peak currents *vs.* the logarithmic scan rates corresponding to this equation: $I_{pa}(\mu A) = 1.0678\log v + 2.6842$ (R^2=0.981). The slope of 1.0678 is clearly close to the theoretical value equal to 1 for an ideal surface absorption mechanism [44]. The plot of $\log I_{pa}$ *vs. E* which is known as the Tafel plot is used to obtain the information on the rate determination phase. This plot was drawn by the use of the increasing section of the guanine's current-potential curve recorded in the scan rate of 0.02 V/s (Fig. 8(c)). This section of the voltammogram which is called the Tafel zone is under the influence of the kinetics of electron transfer between the guanine and the PSSA/NiO/MCM-41/Gr/GCE surface. Therefore, the electron transfer coefficient value can be calculated by the Tafel equation's slope. By the use of the Tafel equation (equation 2) and entering the slope value for the guanine, and with the assumption of its oxidation process being single-electron, the electron transfer coefficient value (α) was calculated as 0.46 [45].

$$E = a - b\log i \quad (2)$$

The calculated value of α for the guanine oxidation being close to the ideal value 0.5 is indicative of ease of electron transfer between the electroactive species of guanine and the modified electrode surface. Fig. 8(d) shows a linear relationship between anodic peak potential and log*v*. Based on the Laviron equation [44], for an irreversible anodic reaction, the anodic peak potential (E_{pa}) is defined as following:

$$E_{pa} = E^{0\prime} + \frac{2.0303RT}{(1-\alpha)nF}\log\frac{(1-\alpha)nF}{RTk_s} + \frac{2.303RT}{(1-\alpha)nF}\log v \quad (3)$$

In the above equation, the terms $E^{0\prime}$,α, *F*, k_s, *and v* are the formal standard potential, electron transfer coefficient, Faraday constant, electron transfer rate constant, and the potential scan rate, respectively. Also, *n* is the number of electrons taking part in the mechanism. The number of electrons transferred in the electrode reaction was estimated directly by using the slope of Eq. 3. Therefore, the number of electrons involved during guanine oxidation reaction in 0.1 M phosphate buffer solution (pH= 5.0) at the surface of PSSA/NiO/MCM-41/Gr/GCE electrode by the use of equations's slope and entering the constant values such as the *F*, *R*, and *T* and α=0.46 was calculated as ≈2. Since the ratio of the number of the involved electrons to the protons in the guanine oxidation reaction is equal to 2, the number of the involved protons was also calculated as ≈1. Therefore, it can be concluded that the guanine oxidation on the modified PSSA/NiO/MCM-41/Gr/GCE is done with the exchange of two electrons and one proton (Fig. 9).

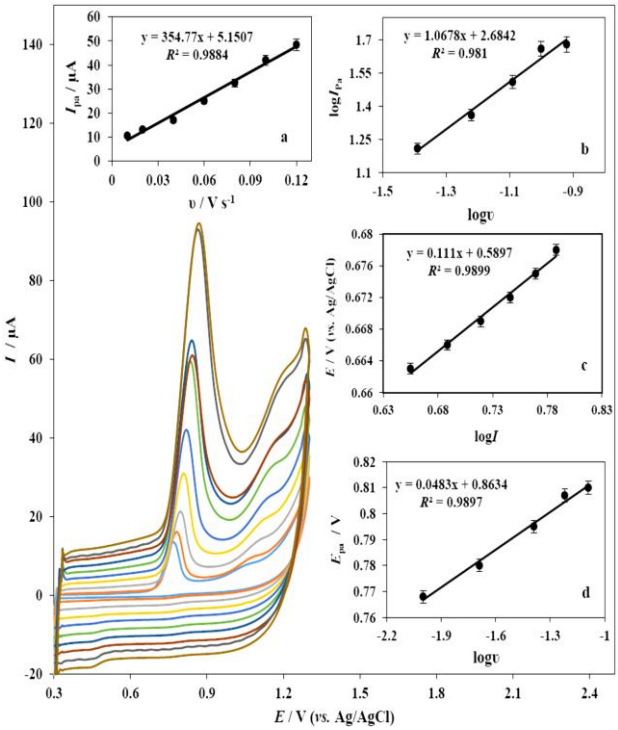


Fig. 8. The cyclic voltammograms of 0.1 M phosphate buffer solution (pH=5.0) containing 10 µM guanine on the PSSA/NiO/MCM-41/Gr/GCE surface at different scan rates over the range of 0.01–0.18 V/s, (a) the linear relationship of the anodic peak current *vs.* scan rate, (b) the linear relationship of the $\log I_{pa}$ *vs.* log*v*, (c) Tafel plot obtained from the current-potential curve recorded in potential rate of 0.02 V s^{-1}, (d) the linear relationship of the E_{pa} *vs.* log*v*.

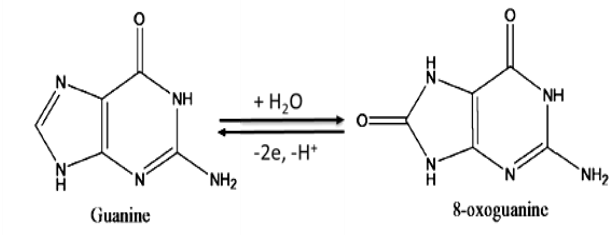


Fig. 9. Proposed electrochemical oxidation mechanism of guanine on the surface of PSSA/NiO/MCM-41/Gr/GCE.

Influence of the time of accumulation (t_{acc}) and potential of accumulation (E_{acc}) of guanine

Since the reaching of the guanine from the solution mass to the electrode surface is an absorption controlled

mechanism, the determination of the optimized time and potential of accumulation is essential for the conduct of the other experiments and increasing the measurement sensitivity. To optimize the accumulation time, before recording the related voltammograms, the modified PSSA/NiO/MCM-41/Gr/GCE was put inside a 10 µM guanine solution with the optimized pH=5.0 for a specified time in the range 0–720 s (Fig. S2(a)). As seen in Fig. S2(b), with the increase in accumulation time from 0 to 360 s, the anodic peak current value is increased and after 360 s, its current response becomes almost constant. Therefore, the optimized accumulation time of 360 s was selected for the next stages. The effects of the accumulation potential on the anodic peak current of 0.1 M phosphate buffer solution (pH=5.0) containing 10 µM guanine over the range of 0.1–0.4 V at t_{acc} of 360 s were investigated (Fig. S2(c)). As is seen in Fig. S2(d), the changes in the accumulation potential is effective on the anodic peak current.

Analytical Performance

The calibration curve was determined under the optimized conditions in the previous phases to investigate the linear dynamic range (LDR) and the LOD of the guanine with the PSSA/NiO/MCM-41/Gr/GCE by differential pulse voltammetry. DPV technique has much higher current sensitivity and better resolution compared to CV technique. Therefore, the DPV method in a wide concentration range was investigated. Fig. 10(a) shows the guanine's DPV in the concentration range of 0.001–36 µM at scan rate of 120 mV/s. As is seen, with the increase in guanine concentration, the DPV oxidation peaks increased gradually. Fig. 10(b) displays the changes of the anodic peak current *vs.* guanine concentration. According to the mentioned figure, the calibration plot of guanine determination was linear over a concentration range of 0.001–36 µM with a regression equation of I_{pa} = 0.977C_G (µM) + 1.432 (R^2 = 0.998). Thus, in this concentration range, guanine has active sites to be absorbed on the PSSA/NiO/MCM-41/Gr/GCE surface [44]. Regarding the slope obtained in the calibration curve, the sensitivity of the modified electrode for guanine is 0.977 µA/µM. The LOD of the proposed modified electrode (PSSA/NiO/MCM-41/Gr/GCE) (C_{LOD}= 3S_b/m, where S_b is the standard deviation obtained from 5 repetition of DPV in the blank solution and m is the sensitivity of the modified electrode in guanine measurement (calibration curve slope)) was 0.5 nM. A comparison between the analytical performance of the present modified electrode and some previous literature electrodes for the determination of guanine is given in Table 1. The results presented in the Table demonstrate that the simultaneous presence of MCM and NiO, along with their synergistic effects, endow the proposed electrode with an extended linear range and an improved detection limit compared to prior literature. As a result, this electrode holds the potential to facilitate the analysis of trace amounts of guanine with enhanced precision and accuracy.

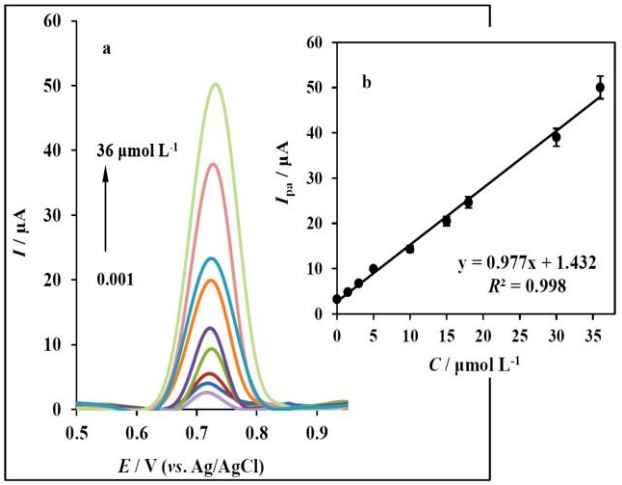


Fig. 10. (a) DPVs of the PSSA/NiO/MCM-41/Gr/GCE in the 0.1 M phosphate buffer solution (pH=5.0) containing guanine in the concentration range of 0.001–36 µM and a scan rate of 0.12 V/s, (b) the calibration curve corresponding to the response of the PSSA/NiO/MCM-41/Gr/GCE to the concentration of guanine.

Table 1
Comparison of the proposed electrode with other electrodes for the determination of guanine

Electrode	Guanine		Method	Ref.
	LDR (µM)	LOD (nM)		
NC-SWCNH/GCE	0.74–6.4	170	LSV	[17]
PPYOX/MWCNTs-MoS2/GCE	10–240	140	SWV	[24]
PDA/MnO2/IL-GR/GCE	10–300	250	DPV	[27]
Graphene-COOH/GCE	0.5–200	50	DPV	[46]
Cu@Ni/MWCNTs/GCE	1.0–180	170	DPV	[47]
PPYOX/GR/GCE	0.04–100	10	LSV	[48]
N-RGO/GCE	0.414–371	138	LSV	[49]
MWCNT-Fe3O4@PDA-Ag/CPE	5–140	1360	DPV	[50]
PSSA/NiO/MCM-41/Gr/GCE	0.001–36	0.5	DPV	This work

NC-SWCNH: Nanocellulose and single-walled carbon nanohorns; PDA: Polydopamine; IL-GR: Ionic liquid functionalized graphene; Graphene-COOH: Carboxylic acid functionalized graphene; MWCNT: Multiwalled carbon nanotube; PP_{YOX}: Overoxidized polypyrrole; N-RGO: Nitrogen-doped reduced graphene oxide.

Evaluation of the PSSA/NiO/MCM-41/Gr/GCE reproducibility, repeatability, and stability

The reproducibility of the PSSA/NiO/MCM-41/Gr/GCE was investigated by the help of DPV and under optimized conditions. To evaluate the reproducibility of the mentioned electrode, three identical electrodes were made in five different days, and the voltammograms of 0.1 M phosphate buffer solution (pH=5.0) containing 10 µM guanine on these electrodes were recorded. The relative standard deviation (RSD) percentage of the results was obtained as 1.8% for guanine, indicating that the mentioned modified electrode has good reproducibility (Fig. S3). For the investigation of the repeatability of the PSSA/NiO/MCM-41/Gr/GCE, five DPV voltammograms of the 0.1 M phosphate buffer solution (pH=5.0) containing 10 µM guanine were recorded and their RSD percentage was obtained as 1.4%. The obtained results show that the modified electrode has good repeatability (Fig. S4). Furthermore, the stability of the PSSA/NiO/MCM-41/Gr/GCE was assessed over a duration of four weeks under laboratory conditions. Throughout this period, a slight decrease in the peak current of guanine (approximately 92.5% of the initial values) was observed. It is proposed that the PSSA/NiO/MCM-41/Gr/GCE electrode exhibits favorable storage stability, as indicated by these findings (Fig. S5).

Interference Effect in the Guanine Measurement

To study the effects of this factor on the guanine measurement, first, the investigation of a few common coexistence compounds (ascorbic acid, glucose, adenine, thymine and alanine) during measuring the 0.1 M phosphate buffer solution (pH=5.0) containing 10 µM guanine on the PSSA/NiO/MCM-41/Gr/GCE with the DPV method was done. In this phase, first, the differential pulse voltammograms of the 0.1 M phosphate buffer solution (pH=5.0) containing 10 µM guanine were recorded and then, a concentration of the intervening species equal to the guanine concentration was added and its differential pulse voltammogram was recorded. Then, its anodic peak current was compared to that of the guanine solution before addition of the intervening species. The addition of the intervening species was continued with higher concentrations and in each phase, its anodic peak current is compared to that of guanine solution before addition of intervening species. If the changes in the anodic peak current after the addition of the intervening species in the optimal conditions are lower than ±10%, the species will not be considered as an intervening species. The endurance limit of a few intervening species has been provided in Table 2. It can be seen from mentioned table that the PSSA/NiO/MCM-41/Gr/GCE showed a quantitative response for guanine. This situation illustrates that the proposed electrode can also be used for the quantitative analysis of guanine in the sample containing high concentration of interferents.

Table 2
Effect of some common interfering species on the determination of 10 µM guanine by DPV.

Interfering species	Tolerance level ratio
Ascorbic acid	20
Glucose	10
Adenine	10
Thymine	8
Alanine	8

Determination of guanine in real samples by the PSSA/NiO/MCM-41/Gr/GCE

To investigate the electroanalytical performance of the modified electrode in the determination of the guanine, the real sample of the fish sperm's DNA was used. The real sample solution was prepared based on the process mentioned in section "Real samples preparation". Under the optimal conditions, the delegate DPV voltammograms for guanine were depicted in Fig. S6(a). This obviously demonstrates that the observed oxidation peak is related to the oxidation of guanine since this peak increases while adding guanine standard solutions. Fig. S6(b) shows a linear relationship between anodic peak current and concentration of guanine. Based on the calculations, it was revealed that the guanine concentration in the fish sperm's DNA sample was 144.48 ± 1.94 mg/L (n=3). The UV-Vis spectroscopy reference method has been used to compare the results obtained from the electrochemical method and investigate the precision and accuracy of the results. The guanine concentration available in the fish sperm's DNA sample was obtained as 146.72 ± 1.43 mg/L (n=3) using the reference method. Therefore, it can be derived that the values obtained by the voltammetric method conforms to those obtained by the spectrophotometric method. The statistic calculations demonstrate nice agreement between the mean values (t-test) and precision (F-test) for the two methods (P = 0.05).

CONCLUSIONS

In the present research, a modified electrode containing NiO/MCM-41 and a polymer layer was designed to prepare sensitive probes by the use of their reinforcing effects on each other by the help of which the electrochemical behavior of the nucleotides bases such as the guanine can be investigated by voltammetry techniques. The incorporation of PSSA, NiO, and MCM-41 adds to the sensor's novelty, with each component contributing specific properties. By optimizing parameters such as electrolyte type, pH, scan rate, accumulation time, and potential, a linear relationship between the guanine concentration and its anodic peak current was established. The linear range for guanine concentration was found to be 0.001–36 µM, with a sensitivity of 0.977 µA/µM and a limit of detection of 0.5 nM. The modified electrode was successfully applied to measure guanine in fish sperm DNA, indicating its

potential for practical use. The method offers advantages such as high precision, ease of experimentation, low cost of equipment, and short experimental time. Overall, this work presents an electrochemical sensor that demonstrates superior performance compared to existing methods, enabling sensitive and selective detection of guanine in DNA samples.

CONFLICTS OF INTEREST

The authors declare that they have no known competing financial interests or personal relationships that could have appeared to influence the work reported in this paper.

DATA AVAILABILITY

The data that support the findings of this study are available within the article and its supplementary material.

ACKNOWLEDGMENT

The authors gratefully acknowledge the financial support from the Guilan University postgraduate program.

REFERENCES

[1] Yu KX, Qiao ZJ, Song WL, Bi S. DNA nanotechnology for multimodal synergistic theranostics. Journal of Analysis and Testing. 2021 Jun;5(2):112-29.

[2] Chen HQ, Yang W, Zuo H, He HW, Wang YJ. Recent advances of DNA hydrogels in biomedical applications. Journal of Analysis and Testing. 2021 Jun;5(2):155-64.

[3] Arvand M, Sanayeei M, Hemmati S. Label-free electrochemical DNA biosensor for guanine and adenine by ds-DNA/poly (L-cysteine)/Fe3O4 nanoparticles-graphene oxide nanocomposite modified electrode. Biosensors and Bioelectronics. 2018 Apr 15;102:70-9.

[4] Leškovskis K, Zaķis JM, Novosjolova I, Turks M. Applications of purine ring opening in the synthesis of imidazole, pyrimidine, and new purine derivatives. European Journal of Organic Chemistry. 2021 Sep 24;2021(36):5027-52.

[5] Ye X, Du Y, Duan K, Lu D, Wang C, Shi X. Fabrication of nano-ZnS coated PEDOT-reduced graphene oxide hybrids modified glassy carbon-rotating disk electrode and its application for simultaneous determination of adenine, guanine, and thymine. Sensors and Actuators B: Chemical. 2014 Nov 1;203:271-81.

[6] Kalaiyarasi J, Pandian K, Ramanathan S, Gopinath SC. Graphitic carbon nitride/graphene nanoflakes hybrid system for electrochemical sensing of DNA bases in meat samples. Scientific Reports. 2020 Jul 30;10(1):12860.

[7] Arvand M, Mazhabi RM, Niazi A. Simultaneous determination of guanine, adenine and thymine using a modified carbon paste electrode by TiO2 nanoparticles-magnesium (II) doped natrolite zeolite. Electrochimica Acta. 2013 Feb 1;89:669-79.

[8] Ensafi AA, Jafari-Asl M, Rezaei B, Allafchian AR. Simultaneous determination of guanine and adenine in DNA based on NiFe2O4 magnetic nanoparticles decorated MWCNTs as a novel electrochemical sensor using adsorptive stripping voltammetry. Sensors and Actuators B: Chemical. 2013 Feb 1;177:634-42.

[9] Yari A, Derki S. New MWCNT-Fe3O4@ PDA-Ag nanocomposite as a novel sensing element of an electrochemical sensor for determination of guanine and adenine contents of DNA. Sensors and Actuators B: Chemical. 2016 May 1;227:456-66.

[10] Hu J, Xu W, Yang H, Mu L. Uric acid participating in female reproductive disorders: a review. Reproductive Biology and Endocrinology. 2021 Apr 27;19(1):65.

[11] Mazhabi RM, Arvand M. Disposable electrochemical DNA biosensor for environmental monitoring of toxicant 2-aminoanthracene in the presence of chlorine in real samples. Journal of Chemical Sciences. 2014 Jul;126:1031-7.

[12] Ortolani TS, Pereira TS, Assumpção MH, Vicentini FC, de Oliveira GG, Janegitz BC. Electrochemical sensing of purines guanine and adenine using single-walled carbon nanohorns and nanocellulose. Electrochimica acta. 2019 Mar 1;298:893-900.

[13] Thomas B, Matson S, Chopra V, Sun L, Sharma S, Hersch S, Rosas HD, Scherzer C, Ferrante R, Matson W. A novel method for detecting 7-methyl guanine reveals aberrant methylation levels in Huntington disease. Analytical biochemistry. 2013 May 15;436(2):112-20.

[14] Shah M, Patel N, Tripathi N, Vyas VK. Capillary electrophoresis methods for impurity profiling of drugs: A review of the past decade. Journal of Pharmaceutical Analysis. 2022 Feb 1;12(1):15-28.

[15] Takayanagi F, Fukuuchi T, Yamaoka N, Kaneko K. Measurement of the total purine contents and free nucleosides, nucleotides, and purine bases composition in Japanese anchovies (Engraulis japonicus) using high-performance liquid chromatography with UV detection. Nucleosides, Nucleotides & Nucleic Acids. 2020 Dec 1;39(10-12):1458-64.

[16] Arvand M, Ghodsi N. Electrospun TiO2 nanofiber/graphite oxide modified electrode for electrochemical detection of l-DOPA in human cerebrospinal fluid. Sensors and Actuators B: Chemical. 2014 Dec 1;204:393-401.

[17] Feng LJ, Zhang XH, Liu P, Xiong HY, Wang SF. An electrochemical sensor based on single-stranded DNA–poly (sulfosalicylic acid) composite film for simultaneous determination of adenine, guanine, and thymine. Analytical biochemistry. 2011 Dec 15;419(2):71-5.

[18] El-Said WA, Choi JW. Electrochemical Biosensor consisted of conducting polymer layer on gold nanodots patterned Indium Tin Oxide electrode for rapid and simultaneous determination of purine bases. Electrochimica Acta. 2014 Mar 20;123:51-7.

[19] Huang X, Zhu Y, Kianfar E. Nano biosensors: properties, applications and electrochemical techniques. Journal of Materials Research and Technology. 2021 May 1;12:1649-72.

[20] Hu C, Yang DP, Zhu F, Jiang F, Shen S, Zhang J. Enzyme-labeled Pt@ BSA nanocomposite as a facile electrochemical biosensing interface for sensitive glucose determination. Acs Applied Materials & Interfaces. 2014 Mar 26;6(6):4170-8.

[21] Xu J, Li T, Shen S, Zhao L, Ma C, Mahmoud AE, Wang J. Electrochemically reduced carboxyl graphene modified electrode for simultaneous determination of guanine and adenine. Analytical Letters. 2015 Jun 13;48(9):1465-80.

[22] Ansari SH, Arvand M. A magnetic nanocomposite prepared from electrospun CoFe 2 O 4 nanofibers and graphene oxide as a material for highly sensitive determination of rutin. Microchimica Acta. 2020 Feb;187:1-9.

[23] Jeevagan AJ, John SA. Electrochemical sensor for guanine using a self-assembled monolayer of 1, 8, 15, 22-tetraaminophthalocyanatonickel (II) on glassy carbon electrode. Analytical Biochemistry. 2012 May 1;424(1):21-6.

[24] Geng X, Bao J, Huang T, Wang X, Hou C, Hou J, Samalo M, Yang M, Huo D. Electrochemical sensor for the simultaneous detection of guanine and adenine based on a PPyox/MWNTs-MoS2 modified electrode. Journal of The Electrochemical Society. 2019 Apr 12;166(6):B498.

[25] Ferancová A, Rengaraj S, Kim Y, Labuda J, Sillanpää M. Electrochemical determination of guanine and adenine by CdS microspheres modified electrode and evaluation of damage to DNA purine bases by UV radiation. Biosensors and bioelectronics. 2010 Oct 15;26(2):314-20.

[26] Kodakat K, Kumar KG. Development of molecularly imprinted poly (Phenol) membrane based electrochemical sensor for the selective determination of guanine. Journal of The Electrochemical Society. 2022 Mar 21;169(3):037517.

[27] Huang KJ, Niu DJ, Sun JY, Han CH, Wu ZW, Li YL, Xiong XQ. Novel electrochemical sensor based on functionalized graphene for simultaneous determination of adenine and guanine in DNA. Colloids and Surfaces B: Biointerfaces. 2011 Feb 1;82(2):543-9.

[28] Liu T, Zhu X, Cui L, Ju P, Qu X, Ai S. Simultaneous determination of adenine and guanine utilizing PbO2-carbon nanotubes-ionic liquid composite film modified glassy carbon electrode. Journal of Electroanalytical Chemistry. 2011 Feb 1;651(2):216-21.

[29] Tang C, Yogeswaran U, Chen SM. Simultaneous determination of adenine guanine and thymine at multi-walled carbon nanotubes incorporated with poly (new fuchsin) composite film. Analytica chimica acta. 2009 Mar 16;636(1):19-27.

[30] Luo X, Morrin A, Killard AJ, Smyth MR. Application of nanoparticles in electrochemical sensors and biosensors. Electroanalysis: An International Journal Devoted to Fundamental and Practical Aspects of Electroanalysis. 2006 Feb;18(4):319-26.

[31] John A, Benny L, Cherian AR, Narahari SY, Varghese A, Hegde G. Electrochemical sensors using conducting polymer/noble metal nanoparticle nanocomposites for the detection of various analytes: a review. Journal of Nanostructure in Chemistry. 2021 Mar;11:1-31.

[32] Zahra T, Ahmad KS. Structural, optical and electrochemical studies of organo-templated wet synthesis of cubic shaped nickel oxide nanoparticles. Optik. 2020 Mar 1;205:164241.

[33] Tavana T, Rezvani AR, Karimi-Maleh H. Pt-doped NiO nanoparticle-ionic liquid modified electrochemical sensor: a powerful approach for determination of epinine in the presence of phenylephrine as two blood pressure raising drugs. Electroanalysis. 2020 Aug;32(8):1828-33.

[34] Li M, Bo X, Mu Z, Zhang Y, Guo L. Electrodeposition of nickel oxide and platinum nanoparticles on electrochemically reduced graphene oxide film as a nonenzymatic glucose sensor. Sensors and Actuators B: Chemical. 2014 Mar 1;192:261-8.

[35] Hasanzadeh M, Shadjou N, Pournaghi-Azar MH, Jouyban A. Magnetic mesoporous silica: a novel nano-material towards electrochemical sensing. Journal of Electroceramics. 2016 Dec;37:85-91.

[36] Cotolan N, Mureşan LM, Salis A, Barbu-Tudoran L, Turdean GL. Electrochemical detection of lead ions with ordered mesoporous silica–modified glassy carbon electrodes. Water, Air, & Soil Pollution. 2020 May;231:1-8.

[37] Hasanzadeh M, Pournaghi-Azar MH, Shadjou N, Jouyban A. Magnetic nanoparticles incorporated on functionalized mesoporous silica: an advanced electrochemical sensor for simultaneous determination of amiodarone and atenolol. RSC Advances. 2014;4(9):4710-7.

[38] Babaei A, Yousefi A, Afrasiabi M, Shabanian M. A sensitive simultaneous determination of dopamine, acetaminophen and indomethacin on a glassy carbon electrode coated with a new composite of MCM-41 molecular sieve/nickel hydroxide nanoparticles/multiwalled carbon nanotubes. Journal of Electroanalytical Chemistry. 2015 Mar 1;740:28-36.

[39] Abalyaeva VV, Nikolaeva GV, Kabachkov EN, Kiseleva SG, Orlov AV, Efimov ON, Karpacheva GP. Obtainment and comparative study of electrochemical behavior of composite electrodes based on polyaniline and its N-substituted derivatives. Polymer Science, Series B. 2018 Nov;60:780-8.

[40] Bard AJ, Faulkner LR, White HS. Electrochemical methods: fundamentals and applications. John Wiley & Sons; 2022 May 3.
[41] Song Y, Xu Z, Yu X, Shi X, Jiang H, Li X, Kong Y, Xu Q, Chen J. Raspberry-like bismuth oxychloride on mesoporous siliceous support for sensitive electrochemical stripping analysis of cadmium. Molecules. 2017 May 13;22(5):797.
[42] Dube A, Malode SJ, Alodhayb AN, Mondal K, Shetti NP. Conducting polymer-based electrochemical sensors: Progress, challenges, and future perspectives. Talanta Open. 2024 Dec 26:100395.
[43] Ganjeh AA, Arvand M, Habibi MF. Electrostatically self-assembled magnetized MXene/copper ferrite nanospheres hybrids: Evaluation of molecularly imprinted electrochemical sensor for the quercetin antioxidant supplement. Microchemical Journal. 2024 Dec 1;207:112026.
[44] Laviron EJ. General expression of the linear potential sweep voltammogram in the case of diffusionless electrochemical systems. Journal of Electroanalytical Chemistry and Interfacial Electrochemistry. 1979 Jul 25;101(1):19-28.
[45] Wang W, Li R, Zhang R, Ma J, Wang B. Electrocatalytic oxidation of methanol on glassy carbon electrode modified with nickel–manganese salen complexes encapsulated in mesoporous zeolite A. Journal of Electroanalytical Chemistry. 2015 Apr 1;742:110-21.
[46] Huang KJ, Niu DJ, Sun JY, Han CH, Wu ZW, Li YL, Xiong XQ. Novel electrochemical sensor based on functionalized graphene for simultaneous determination of adenine and guanine in DNA. Colloids and Surfaces B: Biointerfaces. 2011 Feb 1;82(2):543-9.
[47] Wang D, Huang B, Liu J, Guo X, Abudukeyoumu G, Zhang Y, Ye BC, Li Y. A novel electrochemical sensor based on Cu@ Ni/MWCNTs nanocomposite for simultaneous determination of guanine and adenine. Biosensors and Bioelectronics. 2018 Apr 15;102:389-95.
[48] Gao YS, Xu JK, Lu LM, Wu LP, Zhang KX, Nie T, Zhu XF, Wu Y. Overoxidized polypyrrole/graphene nanocomposite with good electrochemical performance as novel electrode material for the detection of adenine and guanine. Biosensors and Bioelectronics. 2014 Dec 15;62:261-7.
[49] Song G, Zhang R, Jiang X, Liu F, Liu X. Nitrogen-doped reduced graphene oxide as a sensing platform for detection of guanine and application in cell necrosis. Chemical Papers. 2020 Jan;74:89-98.
[50] Yari A, Derki S. New MWCNT-Fe3O4@ PDA-Ag nanocomposite as a novel sensing element of an electrochemical sensor for determination of guanine and adenine contents of DNA. Sensors and Actuators B: Chemical. 2016 May 1;227:456-66.